2019 IEEE 58th Conference on Decision and Control (CDC)
Palais des Congrès et des Expositions Nice Acropolis
Nice, France, December 11-13, 2019

Combined sequential mobile sensing agent evacuation and state reconstruction in contaminated spatial fields

Michael A. Demetriou

Abstract— **This paper proposes a new evacuation strategy for mobile agents fleeing an indoor environment with a contaminated spatial field. Since the effects of a contaminated field on the mobile agents are cumulative, then a policy ensuring that each agent reaches safety while minimizing the accumulated effects of the spatial field is warranted. While each agent is fleeing towards safety, it is also collecting information on the spatial field along its own escape path. This process information, provided by each evacuating mobile agent, is harnessed for the state reconstruction of the spatial process. Thus, an integrated state estimation scheme with the simultaneous sequential agent evacuation is proposed. Numerical results are included to highlight the proposed evacuation policy.**

I. Introduction

The use of multi-agent methods for control of human crowd, with application to leader selection, evacuation, consensus, has been proven to be an indispensable tool. Interactions with fields, such as contaminated concentration, temperature, electromagnetic, radiation, information etc, has also been incorporated in decision making with partial effects of the field on the decision. The use of robotic sensors for spatial field estimation has been examined in earlier works [1], [2], [3], [4], [5] examining various aspects of the robot motion for field reconstruction. However, when the field effects are cumulative, where accumulated exposure to a field proves detrimental, then a new policy must be implemented.

This work examines the modification to a navigation policy which takes the role of an evacuation problem of mobile agents in indoor environments with contaminated spatial fields. The premise is that prolonged exposure to the contaminated spatial field renders an agent incapacitated; for a human being in a hazardous environment, the exposure is quantified in terms of the amount of the substance inhaled, e.g. carbon monoxide. If the field represents temperature, then prolonged exposure leads to hypothermia or hyperthermia. For an unmanned mobile platform in a toxic environment, the exposure is quantified in terms of the accumulated measurements. For a corrosion-inducing field, prolonged exposure leads to physical destruction.

The use of this accumulated exposure to a spatial field as an augmented state to the equations of motion is made possible via the use of the line integral of the mobile agent along the unknown escape path. This enables the derivation of the escape policy that produces an escape path that is not necessarily a straight path in the indoor environment, and which ensures the accumulated effects are at, or below, a threshold value. This flight to escape path for each agent is harnessed, at no additional burden to the agent's motion, to help with the state estimation of the spatial field. Assuming that each mobile agent is equipped with a sensing device that obtains process information of the spatial field along its own escape path, a state estimation scheme with mobile sensors is then modified to account for the sequential agent evacuation and their utilization as adaptive measurements for the spatial process. This is made possible via the asymptotic embedding of the spatial process into a parabolic partial differential equation with mobile sensors [6]. By the correct scheduling of the agent evacuation, in a sequential fashion, the state of the spatial field can be reconstructed.

This paper addresses the design of the sequential evacuation of mobile agents in an indoor environment with contaminated field, and the simultaneous state reconstruction of the field with mobile sensor measurements via asymptotic embedding methods. Thus the contribution is two-fold:

- provide an escape policy of each agent with the added feature of minimizing the exposure to the field,
- establish a sequential agent evacuation policy harnessing each agent's measurements in order to simultaneously estimate the spatial field

The mathematical modeling of the contaminated field in an indoor environment is presented in Section II along with the equations governing the motion of each agent and the quantification of the accumulated effects of the spatial field via the use of line integrals. Section III summarizes the evacuation motion control for each agent which guarantees that the accumulated exposure to the field falls below a given value. The proposed integrated sequential agent evacuation and the state reconstruction of the spatial field is presented in Section IV. Numerical studies examining various aspects of the sequential evacuation of agents in contaminated fields and state reconstruction of the field are presented in Section V.

II. Mathematical modeling and problem formulation

A. Mathematical representation of hazardous field

While the spatial field is represented by the 2D spatial function $c(\xi,\psi)$ defined over a 2D spatial domain $\Omega = [0,L_X]\times[0,L_Y]$, we view it as the solution to an elliptic partial differential equation. This is because the elliptic PDE can be embedded into a parabolic PDE representing the state estimator for $c(\xi,\psi)$, [6]. The spatial process is governed by

$$\mathcal{L}c = f \qquad \text{in } \Omega, \tag{1a}$$

M. A. Demetriou is with Worcester Polytechnic Institute, Dept of Mechanical Engineering, Worcester, MA 01609, USA, mdemetri@wpi.edu.
Research was partially supported through NSF-CMMI, grant # 1825546.

$$c = 0 \text{ on } \Gamma_1, \qquad \frac{\partial c}{\partial \nu} = 0 \text{ on } \Gamma_2. \tag{1b}$$

The solution to (1) is denoted by $c(\xi,\psi)$ and represents the hazardous field. The boundary of the spatial domain $\partial\Omega = \Gamma_1 \cup \Gamma_2$ consists of two disjoint closed sets Γ_1 and Γ_2. The spatial function $f : \Omega \to \mathbb{R}^1$ represents the forcing function in (1a) and it is usually assumed unknown. An unknown function f does not allow the derivation of an analytical solution of the spatial field c. The spatial operator $\mathcal{L}$ is taken to be the second-order (elliptic) differential operator, [7].

Each agent (unmanned mobile platform or human) collects process measurements via a pointwise sensor whose centroid is placed at the mobile agent coordinates $(x_1,x_2) \in \Omega$. Thus the measurement y is given by the value of the spatial field $c(\xi,\psi)$ evaluated at the agent coordinates (x_1,x_2) and equal to $y = c(x_1,x_2)$. If the agent is moving, its position within Ω is given by $(x_1(t),x_2(t))$ and therefore the output measurement is rendered time-varying and given by

$$y(t) = \int_0^{L_X} \int_0^{L_Y} \delta(\xi - x_1(t))\delta(\psi - x_2(t))c(\xi,\psi)\,\mathrm{d}\psi\mathrm{d}\xi. \tag{2}$$

It should be noted that the spatially distributed field $c(\xi,\psi)$ is constant in time and therefore any pointwise measurements at a fixed centroid (x_1,x_2) would be constant. However, as the centroid with coordinates $(x_1(t),x_2(t))$ is moving within Ω, the measurements will be evaluated at different spatial locations thus providing a time-varying output signal $y(t)$.

B. Kinematics of mobile agents

It is assumed that there are N agents to be used for the sequential evacuation and simultaneous state estimation. The motion of each agent is governed by the kinematic equations

$$\begin{aligned} \dot{x}_{1i}(t) &= \upsilon_i \cos(\theta_i(t)), \quad x_{1i}(t_0) = x_{10i}, \\ \dot{x}_{2i}(t) &= \upsilon_i \sin(\theta_i(t)), \quad x_{2i}(t_0) = x_{20i}, \end{aligned} \qquad i = 1,\ldots,N, \tag{3}$$

where υ_i is the speed of the i^{th} mobile agent and $\theta_i(t)$ is the heading angle of the i^{th} agent. Following (2), the output measurement obtained by the i^{th} agent with time-varying coordinates $(x_{1i}(t),x_{2i}(t)) \in \Omega$ is given by

$$y_i(t) = c(x_{1i}(t),x_{2i}(t)), \quad i = 1,\ldots,N. \tag{4}$$

C. Modeling of accumulated effects of the hazardous field

While an agent is traversing the domain Ω obeying (3), it will be collecting process information according to (4). As the effects of the spatial field on the agent (human or hardware) are cumulative, the measure of the accumulated exposure to the field over a given path $\mathbf{C}_i$ of the i^{th} agent in Ω is given by the line integral of the field over the chosen path $\mathbf{C}_i$ [8]. The path $\mathbf{C}_i$ for the i^{th} agent is assumed to be a smooth curve in the plane. For a path commencing at the point $(x_{10i},x_{20i}) \in \Omega$ at the initial time t_0, the accumulated exposure up to the point $(x_{1i}(t),x_{2i}(t))$ at a future time t, is

$$\begin{aligned} \int_{\mathbf{C}_i} c(x_{1i},x_{2i})\ \mathrm{d}\mathbf{s} &= \int_{t_0}^{t} c(x_{1i}(t),x_{2i}(t)) \sqrt{(\mathrm{d}x_{1i})^2 + (\mathrm{d}x_{2i})^2} \\ &= \int_{t_0}^{t} c(x_{1i}(t),x_{2i}(t)) \sqrt{\dot{x_{1i}}^2(t) + \dot{x_{2i}}^2(t)}\,\mathrm{d}t \\ &= \int_{t_0}^{t} c(x_{1i}(t),x_{2i}(t))\upsilon_i\,\mathrm{d}t. \end{aligned}$$

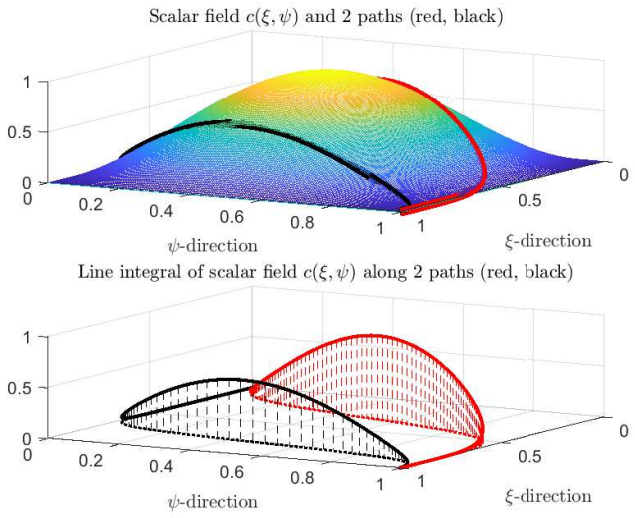

Fig. 1. Example of a path-dependent line integral and the corresponding accumulated amount along the path starting at the origin $(0,0)$ and ending at $(1,1)$; (a) spatial field $c(\xi,\psi) = \sin(\pi\xi)\sin(\pi\psi)$ and two different paths (red and black); (b) area under spatial field along the two paths.

Thus, the accumulated exposure of an agent along a path $\mathbf{C}_i$ from the time t_0 up to time t is given by the line integral

$$\mathcal{E}_i(t;t_0) = \int_{t_0}^{t} c(x_{1i}(t),x_{2i}(t))\upsilon_i\,\mathrm{d}t, \quad i = 1,\ldots,N. \tag{5}$$

D. Problem statement

An agent is assumed to be initially positioned anywhere in the spatial domain Ω including its boundary $\partial\Omega$, and it is desired to reach the origin $(0,0)$. The control problem is to choose the heading angle $\theta_i(t)$ for each agent so that

1) an agent, starting anywhere in Ω with coordinates (x_{10i},x_{20i}), reaches the desired coordinates $(0,0)$,
2) an agent, while traversing Ω to reach $(0,0)$, is also collecting process information via (4),
3) an agent, while traversing Ω to reach $(0,0)$, ensures that the accumulated effects of the spatial field $c(\xi,\psi)$, as quantified by (5), are minimized,
4) an agent, while traversing Ω to reach $(0,0)$, is also helping via (4) to estimate the field $c(\xi,\psi)$ in (1).

E. Discussion of control problems and approaches

Problem 1 is seen to be Zermelo's navigation problem [9]. Problem 2 is a trivial extension to Problem 1 since the i^{th} agent equipped with a sensing device can obtain the time varying measurements (4) along its path described by $\mathbf{C}_i$.

Problem 3 increases the complexity of the navigation problem since now the selected path $\mathbf{C}_i$ must ensure that the accumulated exposure, given via $\mathcal{E}_i$ in (5), is set to an a priori defined value. The solution to this is summarized in Section III. It turns out that it is independent of Problem 4.

Problem 4 can be solved using earlier results on the asymptotic embedding methods for the state estimation of spatially distributed processes [6]. However, in order to account for the evacuation of all N agents in a sequential fashion, a coupling of Problems 3 and 4 is required. This is the main contribution here and is presented in Section IV.

III. Process-dependent navigation: solving Problem 3

The solution to Problem 3 turns out to be a modification to Zermelo's navigation problem [9] and its solution is presented here. The solution will be provided for one agent, but each agent can employ the same solution.

One way to incorporate the accumulated exposure $\mathcal{E}_i$ from (5) to the optimal navigation problem, is to augment (3) with an additional state. Using the isoparametric constraint [10]

$$\int_{t_0}^{t_f} c(x_1(t),x_2(t))\upsilon \,\mathrm{d}t = c_f,$$

with the aid of (5), we arrive at the augmented dynamics

$$\begin{aligned} \dot{x}_1(t) &= \upsilon\cos(\theta(t)),\\ \dot{x}_2(t) &= \upsilon\sin(\theta(t)),\\ \dot{x}_3(t) &= \upsilon c(x_1(t),x_2(t)). \end{aligned} \tag{6}$$

The constant bound c_f denotes the desired level of accumulated exposure of an agent incurred up to the final time t_f. However, it does not provide a closed-form solution. The alternate, is to use the accumulated exposure as the cost; thus the optimization problem becomes

$$\begin{aligned} &\text{minimize} && \int_{t_0}^{t_f} \upsilon c(x_1(t),x_2(t))\,\mathrm{d}t\\ &\text{subject to (6) with} && x_1(t_0)=x_{10},\ x_2(t_0)=x_{20},\\ & && x_1(t_f)=0,\ x_2(t_f)=0. \end{aligned} \tag{7}$$

Lemma 1: The solution to the optimization problem for a single agent satisfying (6) is expressed via the heading angle

$$\dot{\theta} = \upsilon\left[\frac{c_\psi(x_1,x_2)\cos(\theta) - c_\xi(x_1,x_2)\sin(\theta)}{c(x_1,x_2)}\right],$$

Proof: Following the approach in [9] for the solution to the standard navigation problem, we select $\mathbf{L} = \upsilon c(x_1,x_2)$ with $\mathbf{x} = (x_1,x_2)$ resulting in the Hamiltonian

$$\mathbf{H}(\mathbf{x},\boldsymbol{\lambda},\theta) = \lambda_1\upsilon\cos(\theta) + \lambda_2\upsilon\sin(\theta) + \upsilon c(x_1,x_2),$$

where $\boldsymbol{\lambda} = (\lambda_1,\lambda_2)$ denotes the costate vector. The use of $-\dot{\boldsymbol{\lambda}} = \mathbf{H}_{\mathbf{x}}$ produces the costate equations

$$\dot{\boldsymbol{\lambda}} = -\upsilon_i \nabla c(x_1,x_2). \tag{8}$$

Similarly, the stationarity condition $\mathbf{H}_\theta = 0$ produces

$$-\lambda_1\upsilon\sin(\theta) + \lambda_2\upsilon\cos(\theta) = 0.$$

Using the fact that the Hamiltonian $\mathbf{H}$ is not an explicit function of time and thus $\mathbf{H} = 0$ [9], along with the stationarity condition produce the matrix system

$$\upsilon\begin{bmatrix} -\sin(\theta) & \cos(\theta)\\ \cos(\theta) & \sin(\theta)\end{bmatrix}\begin{bmatrix}\lambda_1\\ \lambda_2\end{bmatrix} = \begin{bmatrix} 0\\ -\upsilon c(x_1,x_2)\end{bmatrix}$$

The solution to the costate equations is given by

$$\begin{aligned} \lambda_1 &= -c(x_1,x_2)\cos(\theta),\\ \lambda_2 &= -c(x_1,x_2)\sin(\theta). \end{aligned} \tag{9}$$

Differentiating either of the first two equations in (9) and setting it equal to its counterpart in (8), produces the optimal navigation for an agent

$$\dot{\theta} = \upsilon\left[\frac{c_\psi(x_1,x_2)\cos(\theta) - c_\xi(x_1,x_2)\sin(\theta)}{c(x_1,x_2)}\right], \tag{10}$$

where $c_\xi(x_1,x_2)$ and $c_\psi(x_1,x_2)$ are the spatial gradients of the spatial function $c(\xi,\psi)$ in the ξ and ψ directions, evaluated at the coordinates (x_1,x_2). ■

Remark 1: The control law (10) requires knowledge of the three scalar quantities $c(x_1(t),x_2(t))$, $c_\xi(x_1(t),x_2(t))$, and $c_\psi(x_1(t),x_2(t))$, at each time, which correspond to the value and the derivatives of the spatial function $c(\xi,\psi)$ evaluated at the current location of each agent $(x_1(t),x_2(t))$. Since the navigation policy (10) requires *only* these three scalar quantities and *not* the spatial function $c(\xi,\psi)$ at the entire spatial domain Ω, it then makes the mobile sensor measurements ideal for implementing a state estimator of the spatial process using mobile sensor information [6]. In other words, one *does not need* the knowledge of the spatial field $c(\xi,\psi)$ everywhere in the spatial domain in order to escape, but only at the locations along each escape path $\mathbf{C}$.

IV. Asymptotic embedding methods for the simultaneous state reconstruction of (1) and sequential evacuation of N mobile agents

The output (4) of each mobile agent whose motion is described by (3), (10), can be used to reconstruct the state of the spatial process in (1). However, if the same motion parameters are used by all mobile agents, then their resulting paths $\mathbf{C}_i$ within the spatial domain Ω will be identical, adding little information to a state estimator. As a solution, each escaping mobile agent can implement (10) with different parameters to ensure different paths $\mathbf{C}_i$ which will enable them to provide more useful information to the state estimator. Thus, each mobile agent will implement (10) in a sequential fashion and with their initial times given by

$$t_{0i} = \sum_{k=1}^{i-1}\left(t_{fk} - t_{0k}\right),\ \ i = 2,\ldots,N, \qquad t_{01} = t_0. \tag{11}$$

The PDE in (1) can be written in an abstract form as

$$0 = \mathcal{A}z + f \tag{12}$$

where $z(\boldsymbol{\xi})$, $\boldsymbol{\xi} = (\xi,\psi)$, denotes the state of the algebraic equation (12) and the operator $\mathcal{A}$ is the abstract representation of (the negative of) the operator $\mathcal{L}$ in (1). The information on the boundary conditions is absorbed in the definition of the operator $\mathcal{A}$ and its domain [11]. With regards to the specific spatial function $c(\xi,\psi) = \sin(\pi\xi/L_X)\sin(\pi\psi/L_Y)$ considered here, the operator $\mathcal{A}$ may be taken as

$$\mathcal{A}\phi = \Delta\phi, \quad \phi \in H_0^1(\Omega),$$

with $f(\boldsymbol{\xi}) = \lambda^2\sin(\pi\xi/L_X)\sin(\pi\psi/L_Y)$, $\lambda^2 = \frac{\pi^2}{L_X^2} + \frac{\pi^2}{L_Y^2}$ or, as

$$\mathcal{A}\phi = \Delta\phi + \lambda^2\phi, \quad \phi \in H_0^1(\Omega),$$

with $f(\boldsymbol{\xi}) = 0$. Following [6] the process (12) is embedded in a parabolic PDE in order to derive its state estimator. The process (12) is supplemented with the measurements obtained by the i^{th} mobile agent and given by (4). These measurements are abstractly written as

$$y_i(t) = \mathcal{C}_i(t)z, \quad i = 1,\ldots,N, \tag{13}$$

where each output operator $\mathcal{C}_i : H^{-1}(\Omega) \to \mathbb{R}^1$ is given by

$$\mathcal{C}_i\phi = \int_0^{L_X}\int_0^{L_Y} \delta(\xi - x_{1i})\delta(\psi - x_{2i})\phi(\xi,\psi)\,\mathrm{d}\psi\mathrm{d}\xi.$$

Following [6], the corresponding state estimator is given by

$$\dot{\widehat{z}}(t) = \mathcal{A}\widehat{z}(t) + f + \mathcal{K}_i(t)\left(y_i(t) - \mathcal{C}_i\widehat{z}(t)\right), \quad \widehat{z}(0) = 0. \quad (14)$$

The filter gain operator $\mathcal{K}_i : \mathbb{R}^1 \to H_0^1(\Omega)$ can be selected using the Kalman filter or the Luenberger observer designs, [6]. In terms of the PDE representation, the process (1) is

$$\begin{aligned} 0 &= \frac{\partial^2 c(\xi,\psi)}{\partial\xi^2} + \frac{\partial^2 c(\xi,\psi)}{\partial\psi^2} + \lambda^2 c(\xi,\psi), \\ c(\xi,\psi)\Big|_{\partial\Omega} &= 0. \end{aligned} \quad (15)$$

The process measurement (4) obtained by the i^{th} agent whose motion is governed by (3) and (10), is given by

$$y_i(t) = c(x_{1i}(t), x_{2i}(t)), \quad i = 1,\ldots,N. \quad (16)$$

The associated state estimator is given by

$$\begin{aligned} \frac{\partial\widehat{c}(t,\xi,\psi)}{\partial t} &= \frac{\partial^2\widehat{c}(t,\xi,\psi)}{\partial\xi^2} + \frac{\partial^2\widehat{c}(t,\xi,\psi)}{\partial\psi^2} + \lambda^2\widehat{c}(t,\xi,\psi) \\ &+ \kappa_i(\xi,\psi;x_{1i}(t),x_{2i}(t))\Big(y_i(t) - \widehat{c}(t,x_{1i}(t),x_{2i}(t))\Big) \quad (17) \\ \widehat{c}(t,\xi,\psi)\Big|_{\partial\Omega} &= 0, \quad \widehat{c}(0,\xi,\psi) = 0. \end{aligned}$$

The function $\widehat{c}(t,\xi,\psi)$ is the state of the estimator and denotes the estimate of $c(\xi,\psi)$ with $\widehat{z}(t) = \widehat{c}(t,\cdot,\cdot)$. The filter kernel $\kappa_i(\xi,\psi;x_{1i}(t),x_{2i}(t))$ depends on both the spatial variables (ξ,ψ) and the i^{th} sensor coordinates $(x_{1i}(t),x_{2i}(t))$. It is the kernel representation of $\mathcal{K}_i^*$.

A modification to (17) with the mobile sensor governed by (6) and navigation (10) is required in order to ensure that the estimator (17) can learn about the spatial process (1). When the i^{th} agent implements the navigation (10) with the same speed υ_i and the same initial pose $\theta_i(0)$, then it will have the same path as the rest of the mobile agents, as demonstrated in Figure 1. In order to ensure that a different path is attained by the i^{th} mobile agent, thus enhancing the learning capabilities of the state estimator (17) and, at the same time ensuring that each accumulated exposure $\mathcal{E}_i(t)$ in (5) is minimized, a coordinated scheduling of the escaping mobile agents is required. This is summarized in Algorithm 1.

Remark 2: Algorithm 1 can also handle the case where the agents can start anywhere in the domain Ω and have different initial conditions, i.e. $(x_{1i}(t_{0i}),x_{2i}(t_{0i})) \neq (x_{1j}(t_{0j}),x_{2j}(t_{0j}))$. However, it must be ensured that the sequential evacuation is maintained, i.e. once the i^{th} agent reaches the origin, then and only then the next agent can commence its own escape flight. In this case, the trajectories $\mathbf{C}_i$ will be different even with the same speeds υ_i.

Remark 3: When mobile agents are deployed in the sequential evacuation following different paths $\mathbf{C}_i$ due to different υ_i and $\theta_i(t_{0i})$, their terminal times will not be identical and consequently the durations $t_{fi} - t_{0i}$ will not be the same.

V. Numerical studies

The process is represented by (14) and whose solution is $c(\xi,\psi) = \sin(\pi\xi/L_X)\sin(\pi\psi/L_Y)$ defined in the domain $\Omega = [0,5]m \times [0,2]m$. This function represents the contaminated field and prolonged exposure to it has detrimental effects.

Algorithm 1 Coordination of sequential evacuation of mobile agents and simultaneous estimation of the hazardous process (1)

1: Initialize $i = 1$
2: Use the i^{th} mobile agent governed by (6) and implement the motion control (10) using a unique set of initial pose $\theta_i(t_{0i})$ and constant velocity υ_i, starting at $(x_{1i}(t_{0i}),x_{2i}(t_{0i}))$ with t_{0i} given by (11) and terminating at the desired $(x_{1i}(t_{fi}),x_{2i}(t_{fi})) = (0,0)$.
3: Use the i^{th} mobile sensor measurements $y_i(t)$ in (4) in the state estimator (17) for the interval $[t_{0i},t_{fi})$.
4: At the completion of the flight of the i^{th} mobile agent to safety in $t_{fi} - t_{0i}$ time units, select another mobile agent by setting $i \longleftarrow i+1$ with different set of $\theta_i(t_{0i})$ and constant υ_i, starting at $(x_{1i}(t_{0i}),x_{2i}(t_{0i}))$ and terminating at the desired coordinates $(x_{1i}(t_{fi}),x_{2i}(t_{fi})) = (0,0)$.
5: Terminate if $i = N$, otherwise goto step 3.

A. Sensitivity study: Effects of initial pose and velocity on optimal navigation (10) and accumulated exposure (5)

As mentioned in Algorithm 1, one way to obtain different trajectories of the agents (6) with optimal navigation (10) is to implement either different initial values of $\theta_i(t_{0i})$ or different constant velocities υ_i, $i = 1,\ldots,N$. The use of different initial positions $(x_{1i}(0),x_{2i}(0))$ is not explored here since the thrust is on the evacuation procedure with learning capabilities of the evacuating mobile agents. However, the sequential evacuation of multiple mobile agents with different initial locations along with the integrated state estimation of the contaminated field can still be handled by the proposed scheme. All agents for this study start from the same spatial location, taken to be $(x_{1i}(0),x_{2i}(0)) = (4.5,2)$, $i = 1,\ldots,N$, and reach safety, taken here to be the origin $(x_{1i}(t_{fi}),x_{2i}(t_{fi})) = (0,0)$, $i = 1,\ldots,N$. The use of identical paths will not enhance the learning capabilities of the state estimator (16) since the full state along $\mathbf{C}_1$ is would have been already considered known. Note that the final times t_{fi} are not identical because the parameters $\theta_i(0)$ and υ_i are not the same for the mobile agents.

1) Effects of initial pose $\theta_i(t_{0i})$: For the first study here, the initial pose $\theta_i(t_{0i})$ was used to examine its effects on both the flight duration (i.e. time to reach safety) and the accumulated exposure (5) with $N = 3$. All three initial times were taken to be $t_{0i} = 0$. A constant speed of $\upsilon_i = 1$ m/s was used for all three agents. The initial pose was selected as $\theta_i(0) = \tan_2^{-1}(x_{2i}(t_f) - x_{2i}(0), x_{1i}(t_f) - x_{1i}(0)) + (i-1)\pi/40$, $i = 1,2,3$. Figure 2a depicts the three different trajectories and the contours of the spatial field $c(\xi,\psi)$, and Figure 2b depicts the accumulated exposure $\mathcal{E}_i(t)$ vs time.

The results are also summarized in Table I. The accumulated exposure at t_{fi} decreases with increasing $\theta_i(0)$. The time to reach safety, given by $t_{fi} - t_{0i} = t_{fi}$, is increasing with increasing initial pose $\theta_i(0)$, since the line integrals (distance covered), as seen in Figure 2, are also increasing.

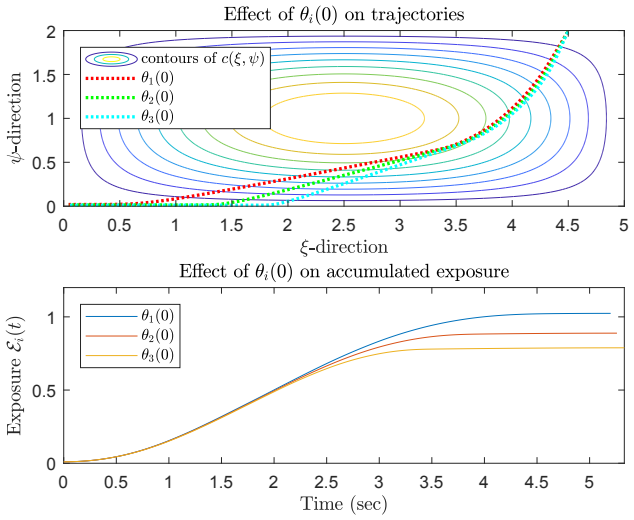

Fig. 2. Case A.1: (a) Effects of $\theta_i(0)$, $i=1,2,3$ on escape trajectory; (b) Effects of $\theta_i(0)$, $i=1,2,3$ on accumulated exposure.

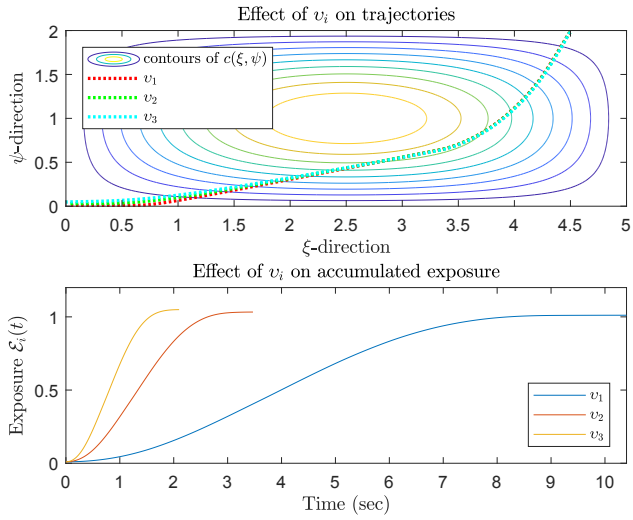

Fig. 3. Case A.2: (a) Effects of υ_i, $i=1,2,3$ on escape trajectory; Effects of υ_i, $i=1,2,3$ on accumulated exposure.

Increasing initial pose essentially forces the trajectories to "curve-outward" thus covering a larger distance.

TABLE I

EFFECTS OF INITIAL POSE $\theta_i(0)$ ON FLIGHT DURATION t_{fi} AND ACCUMULATED EXPOSURE $\mathcal{E}_i(t)$.

initial pose $\theta_i(0)$	flight duration t_{fi}	exposure $E_i(t_{fi})$
$\tan^{-1}\left(\frac{x_{21}(t_f)-x_{21}(0)}{x_{11}(t_{f1})-x_{11}(0))}\right)$	5.20s	1.0239
$\tan^{-1}\left(\frac{x_{22}(t_f)-x_{22}(0)}{x_{12}(t_{f2})-x_{12}(0))}\right)+\frac{\pi}{40}$	5.26s	0.8887
$\tan^{-1}\left(\frac{x_{23}(t_f)-x_{23}(0)}{x_{13}(t_{f3})-x_{13}(0))}\right)+\frac{2\pi}{40}$	5.33s	0.7886

2) Effects of speed υ_i: Now, using the initial pose constant for all three mobile agents to $\theta_i(0)=\tan_2^{-1}(x_{2i}(t_f)-x_{2i}(0),x_{1i}(t_f)-x_{1i}(0))$, $i=1,2,3$, the effects of the velocity υ_i on the time of flight and the accumulated exposure (5) are examined. The velocities were selected as $\upsilon_i=0.5+(i-1)$m/s, $i=1,2,3$. Figure 3a depicts the three trajectories and the contours of the spatial field, where it is observed that as the speed υ_i increases, the trajectories "curve-inward" towards the maximum of the spatial field, thus increasing the exposure to higher values of the spatial field and consequently increasing the accumulated exposure. Figure 3b depicts the evolution of $\mathcal{E}_i(t)$. The effects of increasing the speed are more prominent in the accumulated exposure since the mobile agent accumulates the same amount in shorter time. This is also observed in Table II, where the time of flight decreases with increasing speed.

TABLE II

EFFECTS OF SPEED υ_i ON FLIGHT DURATION t_{fi} AND ACCUMULATED EXPOSURE $\mathcal{E}_i(t)$.

speed υ_i	flight duration t_{fi}	exposure $E_i(t_{fi})$
0.5	10.4s	1.0111
1.5	3.47s	1.0329
2.5	2.10s	1.0493

B. Sequential evacuation of escaping mobile agents and integrated state estimation of hazardous spatial field

As a conclusion to the first study, the speed is selected as $\upsilon_i=1$m/s for all mobile agents in the sequential evacuation and integrated state estimation. To differentiate the trajectories of the agents, which in turn improve the learning capabilities of the state estimator, the initial pose was selected as the discriminating feature of the agents in their path to safety. Alternatively, as per Remark 2, different initial conditions can be used and thus there will be no need to use the speed as the discriminating parameter in order to generate different trajectories $\mathbf{C}_i$. A total of $N=16$ mobile agents were used.

To simulate the state estimator (17), a finite-element based approximation scheme was implemented. To implement the space discretization, 11 linear elements, modified to account for the boundary conditions, were used in each spatial direction [12]. To obtain the matrix representations of the state $\mathcal{A}$ and output operators $\mathcal{C}_i$ in (12), (17), a composite two-point Gauss-Legendre quadrature [13] was used. The system of differential equations was subsequently integrated numerically over the time interval $[0,94]$s using the Matlab® stiff differential equation solver `ode23s`.

The performance of the estimator (16) is quantified in terms of the state estimation error $L_2(\Omega)$ norm given by

$$\|e(t)\|^2_{L_2(\Omega)}=\int_0^{L_X}\int_0^{L_Y}\left(c(\xi,\psi)-\widehat{c}(t,\xi,\psi)\right)^2\,\mathrm{d}\psi\mathrm{d}\xi.$$

The evolution of the error norm is depicted in Figure 4a, where it is observed that with the use of the sequential evacuation of the mobile sensors, the error converges to zero. Additionally, the case of the state estimator utilizing an immobile sensor fixed at $(0.5L_X,0.5L_Y)$ is included. The error norm in this case is also converging to zero, but the case of multiple mobile sensors has a slightly better performance. The individual accumulated exposure functions $\mathcal{E}_i(t)$ commencing at their associated initial times t_{0i} and terminating at their final times t_{fi} are depicted in Figure 4b.

The different paths are superimposed on the top view of

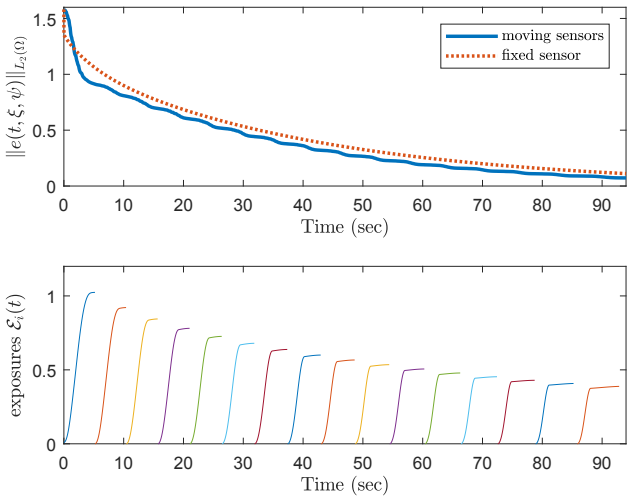

Fig. 4. Case B: (a) Evolution of L_2 state error norm; (b) accumulated exposure of the escaping agents.

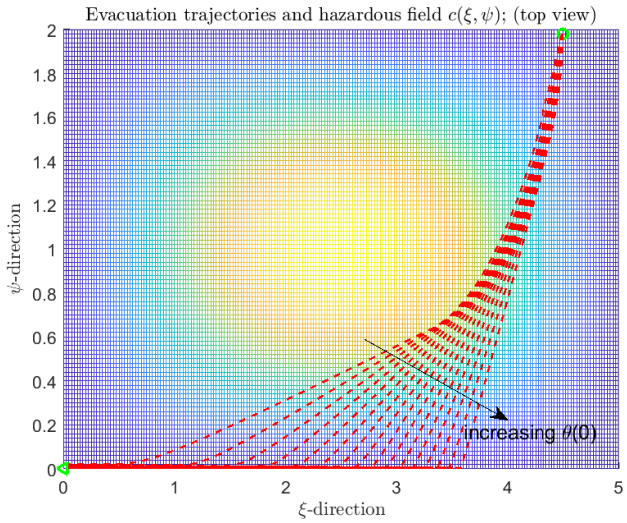

Fig. 5. Case B: Spatial field (top view) and the escaping paths as function of initial pose $\theta_i(t_{0i})$, $i=1,\ldots,N$.

the spatial field and depicted in Figure 5. As established earlier, increasing the initial $\theta_i(t_{0i})$ forces the trajectories to "curve-outward" away from the higher levels of the field. As expected, as the trajectories curve outward, the mobile agents are exposed to lower levels of the field, thus acquiring reduced accumulated levels. These are also tabulated in Table III. It is interesting to note that the flight duration for the trajectories that curve outward is much larger.

VI. Conclusions

An integrated escape policy for mobile agents in indoor contaminated fields that takes into account the cumulative effects of the environment on the health status of the agents has been presented. These effects turned out to be described by the line integral of the unknown spatial field over the unknown escape path. The proposed escape paths had the additional property that knowledge of the entire spatial field was not required, but only along the unknown escape path.

TABLE III

Initial times of sequential agent escape and flight duration.

agent	initial time t_{0i}	duration $t_{fi}-t_{0i}$	amount $\mathcal{E}_i(t_{fi})$
1	0s	5.20	1.0143
2	5.20s	5.24	0.9212
3	10.44s	5.29	0.8442
4	15.73s	5.33	0.7809
5	21.06s	5.39	0.7264
6	26.45s	5.45	0.6797
7	31.90s	5.52	0.6380
8	37.42s	5.60	0.6001
9	43.02s	5.69	0.5667
10	48.71s	5.78	0.5351
11	54.49s	5.89	0.5059
12	60.38s	6.02	0.4788
13	66.40s	6.16	0.4535
14	72.56s	6.33	0.4295
15	78.89s	6.98	0.4083
16	85.87s	7.98	0.3891

This provided an opportunity to harness the spatial field information that each mobile agent was obtaining to help estimate the unknown spatial field. Such a state estimation was made possible via asymptotic embedding methods which enable the dynamics of the unknown field be embedded into the parabolic PDE model of the state estimator with mobile sensors. The result was an integrated state reconstruction of spatial fields and a concurrent sequential evacuation policy of mobile sensing agents.

References

[1] E. Fiorelli, N. E. Leonard, P. Bhatta, D. A. Paley, R. Bachmayer, and D. M. Fratantoni, "Multi-auv control and adaptive sampling in monterey bay," *IEEE J. of Oceanic Engineering*, vol. 31(4), pp. 935–948, Oct 2006.

[2] N. K. Yilmaz, C. Evangelinos, N. M. Patrikalakis, P. F. J. Lermusiaux, P. J. Haley, W. G. Leslie, A. R. Robinson, D. Wang, and H. Schmidt, "Path planning methods for adaptive sampling of environmental and acoustical ocean fields," in *Proc. of the IEEE OCEANS conference*, Sept. 18-21 2006, pp. 1–6.

[3] B. Zhang and G. S. Sukhatme, "Adaptive sampling for estimating a scalar field using a robotic boat and a sensor network," in *Proc. of the IEEE International Conference on Robotics and Automation*, April 10-14 2007, pp. 3673–3680.

[4] M. Rahimi, M. Hansen, W. J. Kaiser, G. S. Sukhatme, and D. Estrin, "Adaptive sampling for environmental field estimation using robotic sensors," in *Proc. of the 2005 IEEE/RSJ International Conference on Intelligent Robots and Systems*, Aug. 2-6 2005, pp. 3692–3698.

[5] M. F. Mysorewala, L. Cheded, M. S. Baig, and D. O. Popa, "A distributed multi-robot adaptive sampling scheme for complex field estimation," in *Proc. of the 11th International Conference on Control Automation Robotics Vision*, Dec. 7-10 2010, pp. 2466–2471.

[6] M. A. Demetriou, "Using asymptotic embedding methods for dynamic estimation of spatial fields with mobile sensors," in *Proc. of the IEEE Conf. on Decision and Control*, FL, USA, 17-19 Dec. 2018.

[7] L. C. Evans, *Partial Differential Equations*, 2nd ed. American Mathematical Society, Providence, RI, 2010, vol. 19.

[8] W. Kaplan, *Advanced Calculus*, 3rd ed. Addison-Wesley Publishing Company, Reading, MA, 1984.

[9] A. E. Bryson, Jr. and Y. C. Ho, *Applied Optimal Control*. John Wiley & Sons, New York-London-Sydney, 1975.

[10] R. F. Stengel, *Optimal control and estimation*. Dover Publications, Inc., New York, 1994, corrected reprint of the 1986 original.

[11] J. C. Robinson, *Infinite-dimensional dynamical systems*. Cambridge University Press, Cambridge, 2001.

[12] K. Höllig, *Finite Element Methods with B-Splines*. Philadelphia, PA: SIAM, Frontiers in Applied Mathematics, 2003.

[13] M. A. Celia and W. G. Gray, *Numerical methods for differential equations*. Englewood Cliffs, NJ: Prentice Hall Inc., 1992, fundamental concepts for scientific and engineering applications.